Simulation of Convective Initiation during IHOP_2002 Using the Flux-Adjusting Surface Data Assimilation System (FASDAS)

PETER P. CHILDS, ANEELA L. QURESHI, SETHU RAMAN, KIRAN ALAPATY, ROBB ELLIS, AND RYAN BOYLES

State Climate Office of North Carolina, and Department of Marine, Earth, and Atmospheric Sciences, North Carolina State University, Raleigh, North Carolina

DEV NIYOGI

Departments of Agronomy and Earth and Atmospheric Sciences, Purdue University, West Lafayette, Indiana

(Manuscript received 17 August 2004, in final form 26 May 2005)

ABSTRACT

The Flux-Adjusting Surface Data Assimilation System (FASDAS) uses the surface observational analysis to directly assimilate surface layer temperature and water vapor mixing ratio and to indirectly assimilate soil moisture and soil temperature in numerical model predictions. Both soil moisture and soil temperature are important variables in the development of deep convection. In this study, FASDAS coupled within the fifth-generation Pennsylvania State University–NCAR Mesoscale Model (MM5) was used to study convective initiation over the International H_2O Project (IHOP_2002) region, utilizing the analyzed surface observations collected during IHOP_2002. Two 72-h numerical simulations were performed. A control simulation was run that assimilated all available IHOP_2002 measurements into the standard MM5 four-dimensional data assimilation. An experimental simulation was also performed that assimilated all available IHOP_2002 measurements into the FASDAS version of the MM5, where surface observations were used for the FASDAS coupling. Results from this case study suggest that the use of FASDAS in the experimental simulation led to the generation of greater amounts of precipitation over a more widespread area as compared to the standard MM5 FDDA used in the control simulation. This improved performance is attributed to better simulation of surface heat fluxes and their gradients.

1. Introduction

As reliance on numerical weather prediction models continues to increase, more accurate and detailed data assimilation systems are essential. Data assimilation is based on the concept of combining current and past meteorological data in an explicit dynamical model. Four-dimensional data assimilation (FDDA) is the time-dependent dynamical coupling of various numerical fields with the model's prognostic equations. FDDA provides a logical extension between objective analysis methods and dynamic relationships of atmospheric variables.

Corresponding author address: Prof. Sethu Raman, North Carolina State University, 242 Research III Building, Centennial Campus, Box 7236, Raleigh, NC 27695-7236.
E-mail: sethu_raman@ncsu.edu

At least two types of sequential FDDA are currently used in operational and research models. The first is a process of initializing an explicit prediction model, using subsequent forecast cycles (typically 3–12 h) as a first guess in the static three-dimensional objective analysis, and then repeating this step for future forecasts. This process is used in many current operational forecast models. A second common method of FDDA uses a continuous (i.e., every time step) dynamical assimilation where forcing functions are added to the governing equations to "nudge" the model state toward the observations. This type of FDDA is often used in the research community to study various mesoscale features. Users of the fifth-generation Pennsylvania State University–National Center for Atmospheric Research (Penn State–NCAR) Mesoscale Model (MM5) modeling system frequently use continuous-nudging FDDA. Nudging was initially developed and tested by Kistler (1974) and by Anthes (1974). Refer to Stauffer and

Seaman (1990) for a more detailed review of these techniques.

The Flux-Adjusting Surface Data Assimilation System (FASDAS) has been continuously developed over the last few years (Alapaty et al. 2001a,b,c). FASDAS builds on the works of Mahfouf (1991) and Bouttier et al. (1993). They used the surface layer temperature and humidity to estimate the soil moisture and temperature evolutions in numerical model predictions. These schemes work well, but assume that the largest errors in the simulated surface energy budget are due to errors only in the soil moisture parameter. However, these errors are not always significant, especially during cloudy conditions. Both soil moisture and soil temperature are important variables in the development of deep convection. FASDAS was developed not only to address these issues but also to include direct and indirect assimilation components utilizing the FDDA methodology employed by Stauffer and Seaman (1990). More information on FASDAS can be found in section 3.

The primary goal of this research is to study the impact of FASDAS on numerical simulations of a convective initiation event that occurred during the International H_2O Project (IHOP_2002) over the southern Great Plains (SGP) of the United States. A main objective of the IHOP_2002 study was to obtain more accurate and reliable measurements of humidity to improve forecasts of convection and associated rainfall. In this study, we use FASDAS to develop realistic soil moisture and temperature fields over the IHOP_2002 region to study convective initiation. Surface observations, used in FASDAS, were obtained from the IHOP_2002 hourly surface meteorological composite dataset (available from the IHOP_2002 data archive Web site http://www.joss.ucar.edu/ihop/dm/archive/). Figure 1 shows the locations of all surface meteorological data sites used in this study. Over 250 locations provided meteorological data, including observations of temperature, wind, and moisture.

Two 72-h numerical simulations were performed. A control simulation was run that assimilated all available IHOP_2002 data into the standard MM5 four-dimensional data assimilation. An experimental simulation was completed that assimilated all available IHOP_2002 data into the FASDAS version of MM5. With the dense observational network during the IHOP_2002 study, local surface fields are better defined, allowing for the inclusion of improved feedback between soil moisture heterogeneity and convection in this region. The study period is from 0000 UTC 17 June 2002 through 0000 UTC 20 June 2002. During this period, intense convection occurred at many locations of the IHOP_2002 region.

2. Synoptic review

Weak northwest upper-level flow was present over the IHOP_2002 region on 17 June 2002. The ridge axis was oriented SW–NE across the central Rockies. Sky conditions were clear on the morning of 17 June, with strong southwest winds at the surface. By the afternoon, a deepening surface low over central Colorado helped push an ENE–WSW-oriented dryline from Colorado into NW Kansas. Convection began to occur along this boundary in NW Kansas and the Oklahoma panhandle between 2000 and 2100 UTC on 17 June. Existence of a low-level jet in western Oklahoma and Kansas supported continuing convection to propagate ESE across Kansas overnight.

On 18 June, the region remained under weak northwest flow, becoming more westerly overnight. A dryline boundary, located near Garden City, Kansas, began to drift NNW during the afternoon. Weak convection developed around 2000 UTC over SE Colorado and moved into north-central Kansas during the evening hours. Convection dissipated quickly after local sunset.

The upper-level pattern shifted to a more WSW flow on 19 June. A surface cold front was located near Goodland, Kansas, by late morning. Between 1740 and 1905 UTC, a NNE–SSW-oriented boundary was observed around Goodland, moving toward Colby, Kansas. Convection began in SE Colorado around 2000 UTC, and quickly developed along the boundary in Kansas, propagating eastward overnight.

Figure 2 shows a mesoscale surface analysis over the IHOP_2002 region valid 0000 UTC 18 June 2002. Surface observations are shown in standard meteorological format. A surface dryline, accompanied by a 10°C drop in surface dewpoint temperature, was analyzed over western Kansas and Oklahoma during this period. East of the dryline, boundary layer winds were from the south and southeast near 10 m s^{-1}, while to the west of the dry line, winds were from the north around 5 m s^{-1}. Figure 3 shows a visible satellite image over the IHOP_2002 region valid 0000 UTC 18 June 2002. Deep convection started developing over portions of northern Texas, western Oklahoma, and western Kansas. Cirrus elements associated with the convection were beginning to spread over central Oklahoma and Kansas during this time period.

3. Methods

The control and experimental simulations were completed using version 3.6.2 of the MM5 modeling system. The simulations were identical with the exception of

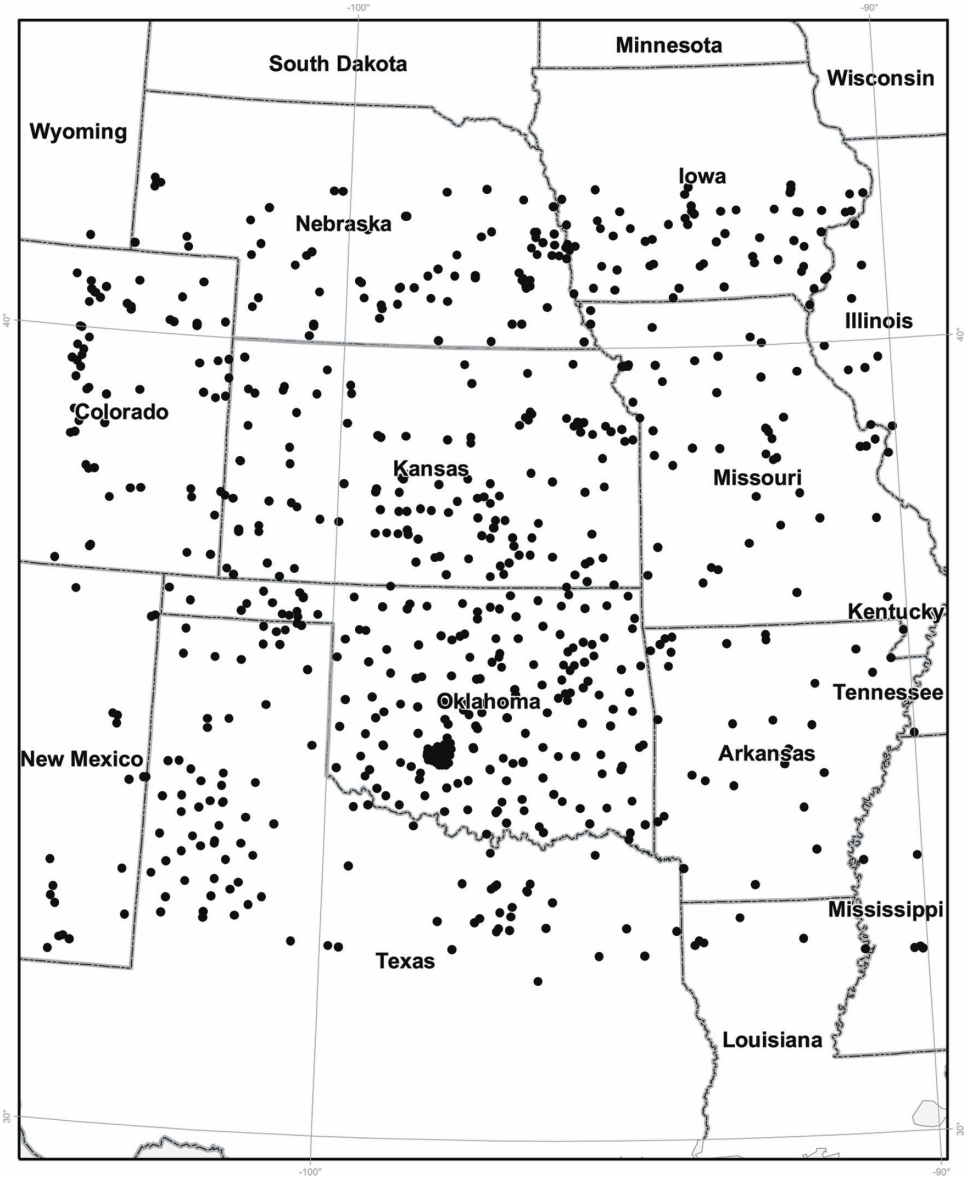

FIG. 1. Map showing the locations of all the mesonet stations included in the IHOP_2002 Hourly Surface Meteorological Composite dataset.

the FASDAS scheme being used in the experimental simulation. The MM5 is the latest version of a mesoscale model first used and developed at the Pennsylvania State University in the early 1970s. MM5 is a primitive equation model that uses a nondimensional terrain-following σ vertical coordinate system. The MM5 modeling system is broken down into three components: 1) main programs, 2) datasets, and 3) additional capabilities. TERRAIN, REGRID, RAWINS, INTERPF, and MM5 are the main programs included in the MM5 model. Programs TERRAIN and REGRID interpolate terrestrial and isobaric atmospheric data in a latitude–longitude mesh to a variable high-resolution model domain. Mesoscale detail is added to the REGRID data with surface and upper-air observations obtained from the IHOP_2002 network of surface and rawinsonde stations incorporated into the LITTLE_R program. The LITTLE_R program was modified to assimilate all available IHOP_2002 meteorological data into the REGRID analysis at 6-h intervals. Atmospheric data are then interpolated from pressure levels to the vertical sigma coordinate system using the INTERPF program. MM5 is the final main program and is the numerical weather prediction component of the

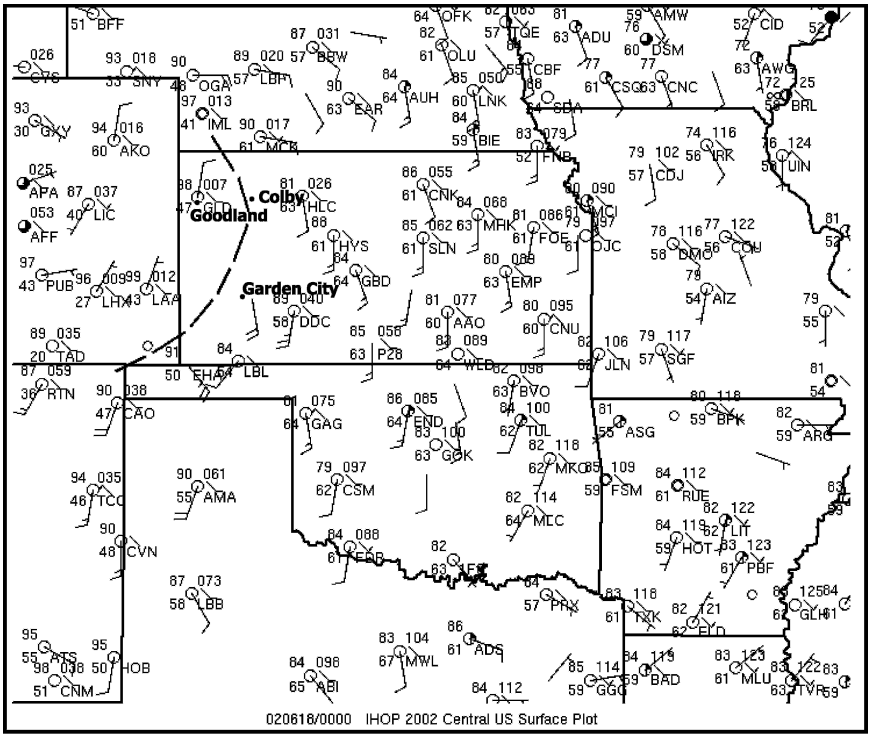

FIG. 2. Surface analysis valid 0000 UTC 18 Jun 2002. Surface observations are shown in standard meteorological format. A surface dryline is highlighted in black above.

model. The MM5 program includes the various physics options and the governing equations.

Eta Model analyses, produced by the National Centers for Environmental Prediction (NCEP) and archived by NCAR were used to prescribe initial and lateral boundary conditions. The resolution of the archived data is approximately 40 km. These analyses are interpolated onto the model grid to serve as initial values and to provide lateral boundary conditions for the simulation. The analysis corresponding to 0000 UTC 17 June 2002 was utilized as the initial condition. The model was integrated up to a period of 72 h, ending 0000 UTC 20 June 2002.

The model simulations for this research used surface layer similarity for the constant flux layer and the Eta Mellor–Yamada (Eta M–Y) planetary boundary layer (PBL) parameterization scheme for the mixed layer (Betts et al. 1997). The Eta M–Y is a 2.5-level 1.5-order turbulent kinetic energy (TKE) closure model used in NCEP's operational Eta Model. The scheme requires a prediction equation for the TKE and parameterization of TKE sources and sinks for each model layer. Prediction of the TKE gives better representation of mixing by subgrid-scale eddies that develop as a result of vertical wind shear. Since the diffusion rates at each model layer in the PBL are determined by the wind, moisture, and temperature conditions at the layer's top and bottom interfaces, the PBL closure is considered to be local. The mixing that is emulated in each time step only takes place through the interface between adjacent model layers. The scheme also requires a soil model that calculates ground temperature at multiple depths.

MM5 uses explicit equations for cloud water, rainwater, ice, and water vapor. The simple ice scheme was used to account for the ice phase processes. In this scheme, there is no supercooled water and immediate melting of snow below the freezing level.

The Kain–Fritsch cumulus parameterization scheme was used to account for the subgrid water cycle (Kain 2004) in the 12-km domain, while the inner 4-km domain used only explicit moisture physics to account for precipitation processes. The Kain–Fritsch parameterization is a complex cloud-mixing scheme that is capable of solving for entrainment and detrainment processes. The scheme also removes the available buoyant energy in the model relaxation time. Updraft and downdraft properties are also predicted. The influence of shear effects on the precipitation efficiency is also considered by the Kain–Fritsch scheme.

The Dudhia cloud-radiation scheme was used to account for the interaction of shortwave and longwave radiation with clouds and the clear air. The scheme provides an important contribution in simulating the

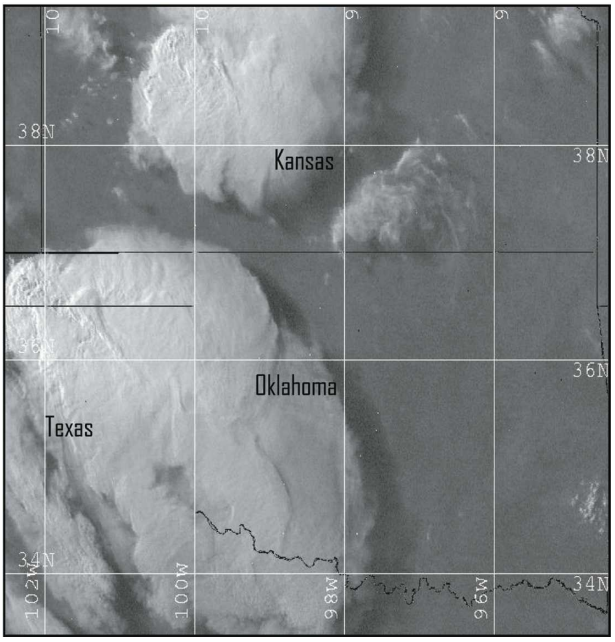

FIG. 3. Visible satellite imagery valid 0000 UTC 18 Jun 2002. States are labeled in black.

atmospheric temperature tendencies. Surface radiation fluxes are also considered in this scheme.

The Noah land surface model (LSM) was used to represent land surface processes. The Noah LSM is one of the recent high-resolution land surface models developed and implemented by research scientists (Ek et al. 2003). The Noah LSM is an updated version of the Oregon State University (OSU) LSM and was fully implemented into the operational Eta Model in spring 2004. Equations for bare soil evaporation and soil thermal conductivity have been revised for use in MM5. In this LSM, soil temperature and soil moisture are predicted at four levels (10, 30, 60, and 100 cm). Soil water/ice, canopy water, and snow cover are also predicted. The soil heat flux explicitly includes contributions from both the snow- and nonsnow-covered portions of a model grid box. This scheme is capable of resolving diurnal air temperature variations that result due to a more rapid response to the surface temperature.

Alapaty et al. (2001c) have developed a technique based on FASDAS that continuously assimilates surface observations to improve surface layer simulations. Forecasted temperature and dewpoint data are compared with interpolated observations. The forecasted temperature and dewpoint are nudged toward the observed values through the adjustment of surface sensible and latent heat fluxes. This in turn alters the surface energy budget and then the soil temperature. This technique was further modified by Alapaty et al. (2001a,b) to include a soil moisture correction.

This technique helps maintain consistency between the ground temperature and soil moisture with the surface-layer mass variables. FASDAS calculates the difference between the observations and model predictions of surface temperature and dewpoint temperature and adjusts surface heat fluxes to account for these differences. These adjustments are added to the surface heat fluxes simulated by the model. The updated heat fluxes are then used in the prognostic ground temperature and soil moisture equations, which in turn affect the simulated surface heat fluxes in the subsequent time step. This process of continuous assimilation occurs throughout the model integration period. For further details refer to Alapaty et al. (2001a,b,c). Preprocessing and analysis packages within MM5 provide an accessible interface for processing. The quality assurance and quality control (QA/QC) for the observations are performed as a part of the preprocessing of the data. A flowchart describing the FASDAS procedure is shown in Table 1.

In the MM5, a preprocessing system provides initial estimates of soil moisture and soil temperature at various depths, water-equivalent snow depth, sea ice, and canopy moisture. These fields are obtained from the Eta Advanced Weather Interactive Processing (AWIP) analyses. Chen and Dudhia (2001) show that much uncertainty still exists in the initial soil moisture estimates,

TABLE 1. Flowchart of the FASDAS procedure.

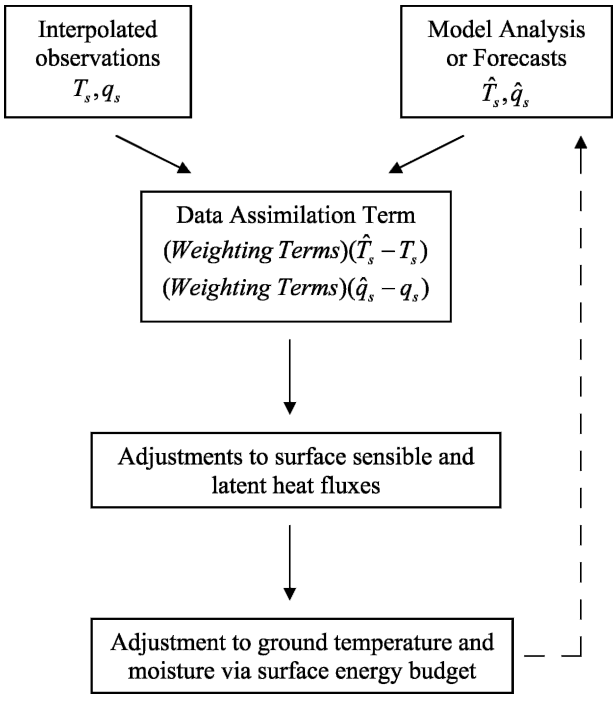

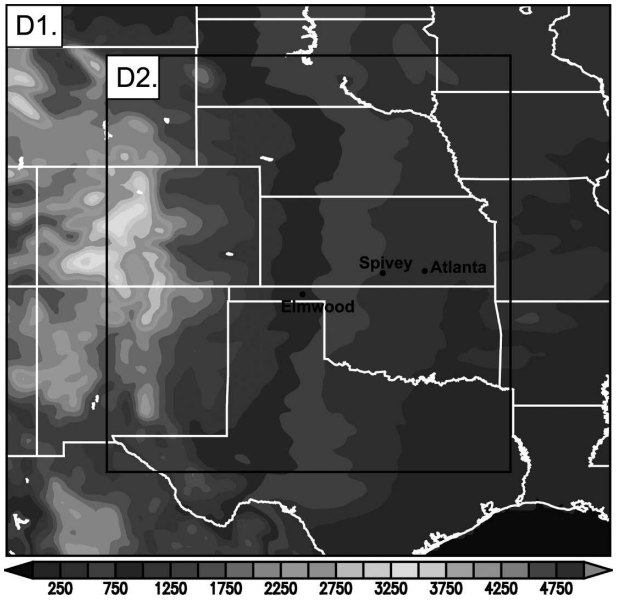

FIG. 4. MM5 domain configuration used in this study. The outer domain, D1, has a horizontal grid spacing of 12 km, while the inner domain, D2, has a horizontal grid spacing of 4 km. Elevation data are shaded in m. Locations of interest are shown in black.

which in turn contributes to model prediction errors. Alapaty et al. (2001a,b) demonstrate how FASDAS corrections for soil moisture and soil temperature can significantly improve model forecasts and reduce errors. For example, using FASDAS, the rms errors for PBL height over the First International Satellite Land Surface Climatology Project (ISLSCP) Field Experiment (FIFE) region in the Great Plains were reduced from 405 to 155 m (Alapaty et al. 2001c). Similarly, Alapaty (2001a,b) reported consistent improvements in model-estimated soil temperature and soil moisture, which led to improvements in model-simulated dewpoint temperature, lifting cloud level, cumulus convection, and precipitation. Therefore, initial studies indicate that the MM5–FASDAS coupling improves model performance by enhancing land–atmosphere feedbacks. For the experimental simulation described here, MM5 was altered to allow for the full implementation of the FASDAS scheme. The code was modified to allow for observational nudging of the mass fields, and to allow for direct interaction between atmospheric variables and related surface fluxes. Observational nudging is prescribed at an interval of 180 min throughout the 72-h model integration.

4. Results and discussion

The main goal of this study is to investigate the effect of using FASDAS on simulated convective initiation over the SGP during the IHOP_2002 experiment. Figure 4 shows the MM5 domain configuration used in this study. The outer domain, D1, has a horizontal grid spacing of 12 km, while the inner domain, D2, has a horizontal grid spacing of 4 km. Elevation data in meters are shaded in Fig. 4 and range from less than 250 m over Kansas and Oklahoma to nearly 3750 m over Colorado. Locations of interest in this study are indicated on Fig. 4. These were the locations where convective activity occurred during the study period.

Surface heat fluxes for Atlanta, Kansas; Elmwood, Oklahoma; and Spivey, Kansas, valid 0000 UTC 17 June through 0000 UTC 20 June 2002, are shown in Figs. 5, 6, and 7, respectively. For each of these figures, surface sensible heat fluxes (W m^{-2}) are shown in (a) and surface latent heat fluxes (W m^{-2}) are shown in (b). These three sites are in the IHOP_2002 domain and are part of the NCAR Integrated Surface Flux Facility

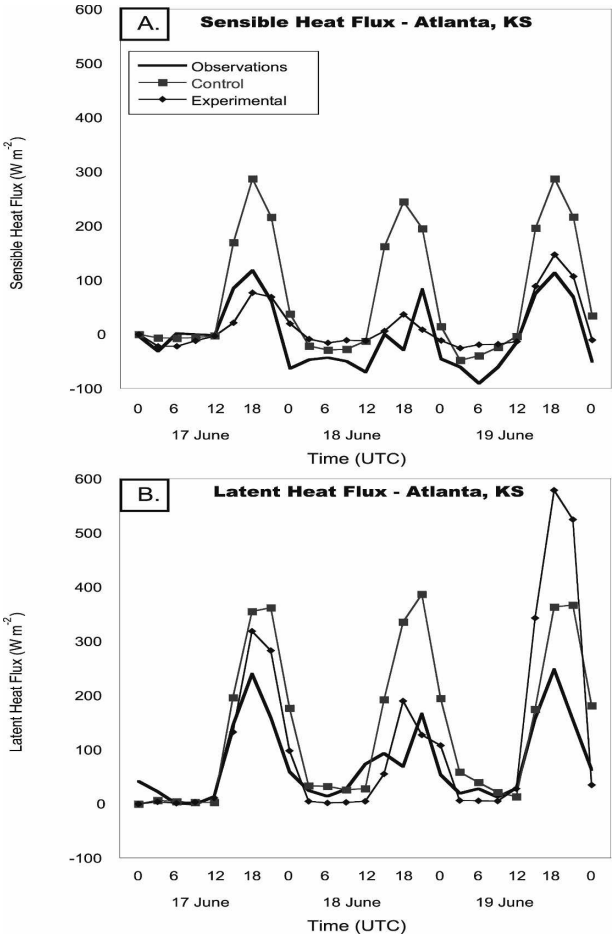

FIG. 5. (a) Simulated surface sensible heat fluxes (W m^{-2}) valid 0000 UTC 17 Jun–0000 UTC 20 Jun 2002 for Atlanta, KS. (b) Simulated surface latent heat fluxes (W m^{-2}) valid 0000 UTC 17 Jun–0000 UTC 20 Jun 2002 for Atlanta, KS.

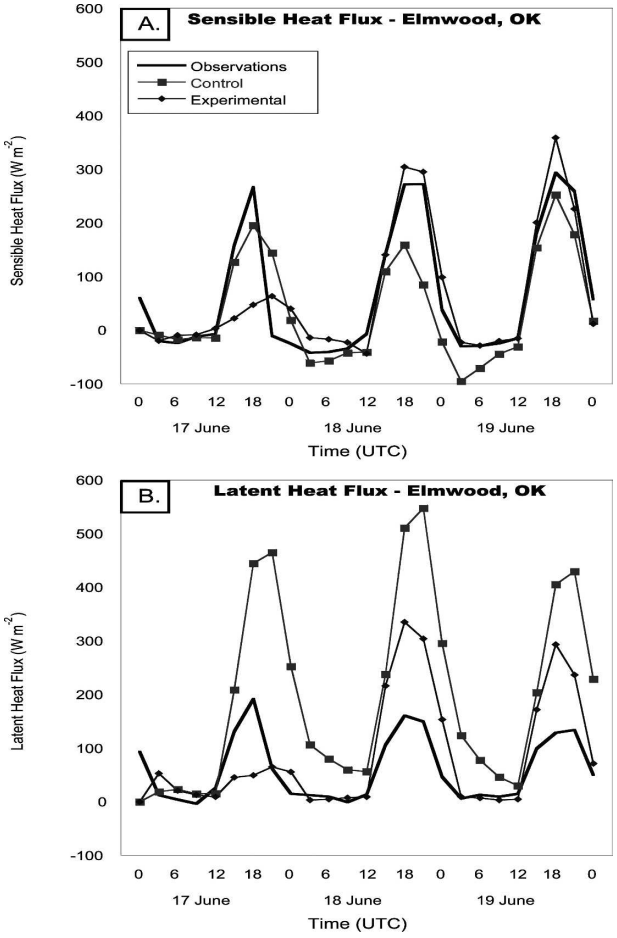

FIG. 6. Same as Fig. 5, except for Elmwood, OK.

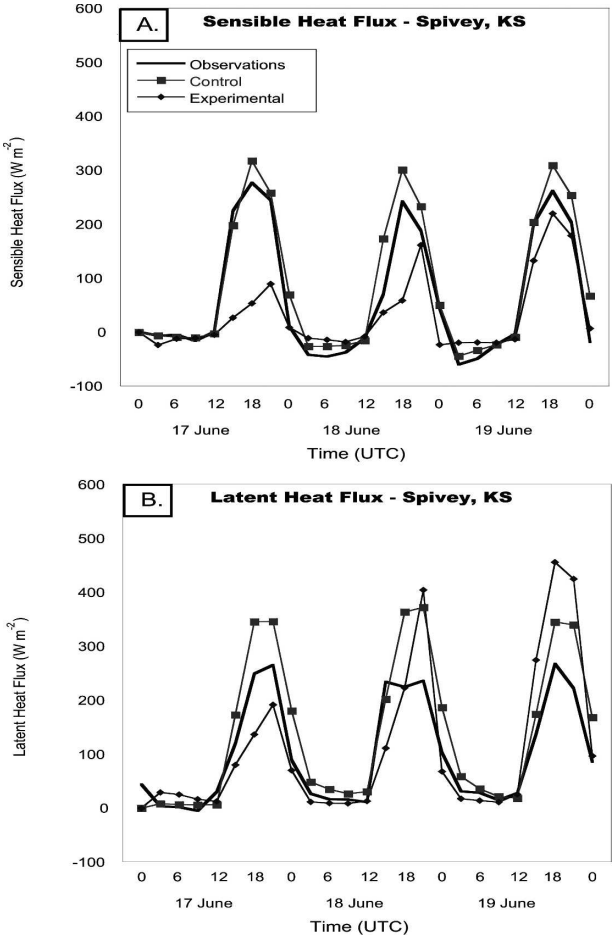

FIG. 7. Same as Figs. 5 and 6, except for Spivey, KS.

(ISFF), which comprises nine surface flux sites located in Kansas, Oklahoma, and Texas. ISFF towers are equipped with sensors to measure fluxes of momentum, sensible and latent heat, trace gases, and radiation in addition to standard surface and atmospheric variables. Observations of surface sensible and latent heat fluxes were used for the comparison purposes in this study. More information on ISFF, including instrumentation and specific variables measured, can be found at http://www.atd.ucar.edu/rtf/projects/ihop_2002/isff/report.shtml.

Figures 5a, 6a, and 7a indicate that the experimental simulation appears to have performed better for the surface sensible heat fluxes. For both Atlanta and Elmwood, the experimental simulated fluxes matched the observations fairly closely over most of the time period. Sensible heat fluxes were underestimated over Spivey in the experimental simulation; however by 19 June they were closer to the observations. The experimental simulation did seem to have problems during the first 24 h of the integration, especially for Elmwood and Spivey, but seemed to perform better in the latter part of the simulation. The control simulation did not perform as well for Atlanta, where fluxes were overestimated throughout the entire simulation, or for Elmwood, where fluxes were underestimated. However, the control simulation performed well for Spivey, where simulated fluxes matched the observations fairly well.

Neither simulation seemed to overall perform better than the other for the surface latent heat fluxes. The experimental simulation came close to observations for Atlanta on 17 and 18 June, but then overestimated fluxes significantly on 19 June. For both Elmwood and Spivey, the experimental simulated latent heat fluxes were underestimated on 17 June, then overestimated for the remainder of the integration. The control simulation consistently overestimated fluxes for all three sites; however for both Atlanta and Spivey the control simulated latent heat fluxes were closer to the observations than the experimental for the final 24 h of the simulation.

Figures 8–14 are valid for 0000 UTC 18 June 2002.

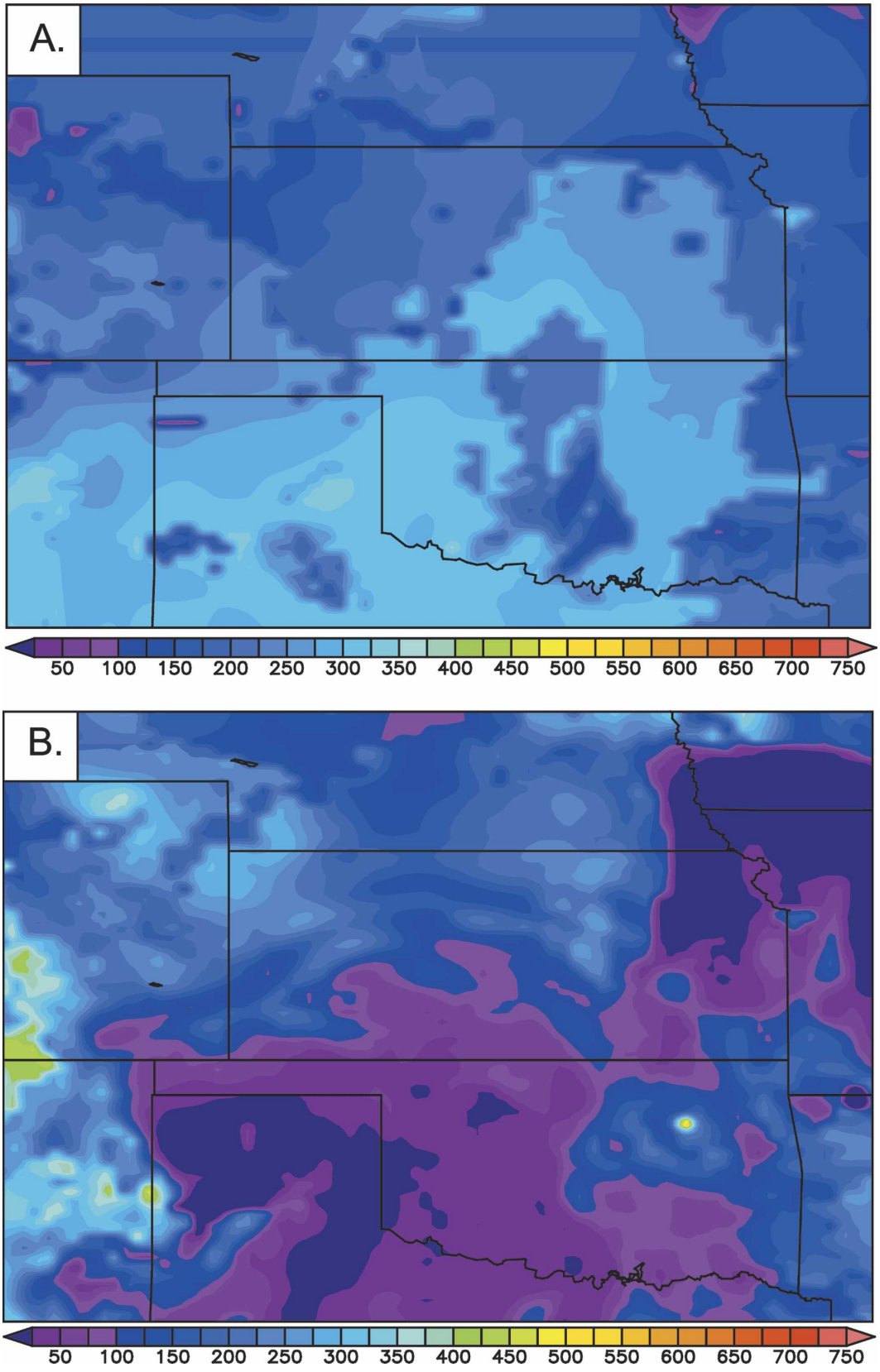

FIG. 8. (a) Control simulated surface sensible heat fluxes (W m^{-2}) valid 0000 UTC 18 Jun 2002. (b) Experimental simulated surface sensible heat fluxes (W m^{-2}) valid 0000 UTC 18 Jun 2002.

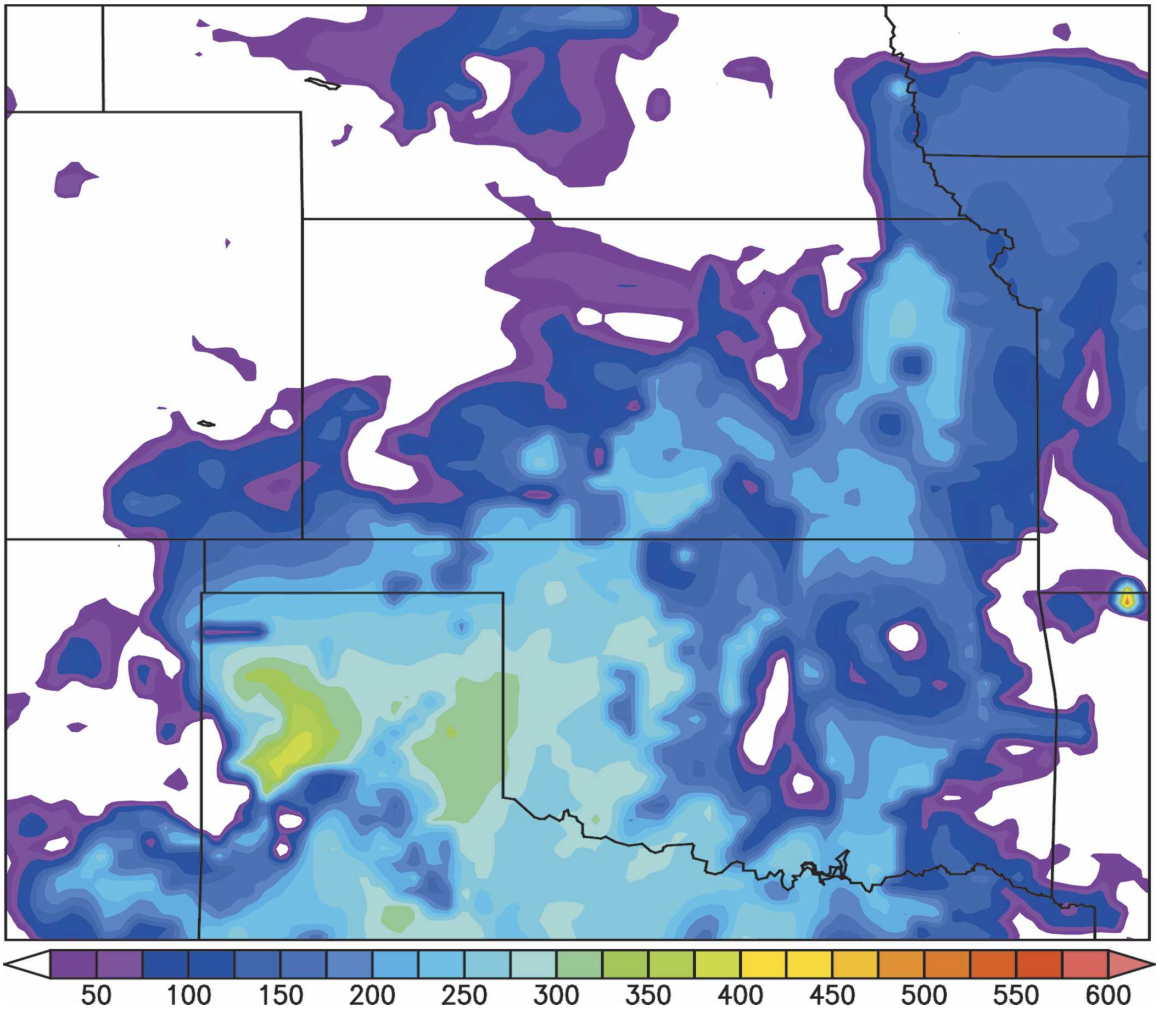

FIG. 9. Numerical difference between the control simulated surface sensible heat flux and experimental simulated surface sensible heat flux valid 0000 UTC 18 Jun 2002. Fluxes are shown in W m^{-2}.

For each of the two figures, (a) is from the control Simulation and (b) is from the experimental simulation. Model-simulated surface sensible heat fluxes (W m^{-2}) are shown in Fig. 8. Sensible heat flux values are fairly uniform over much of the IHOP_2002 region in the control simulation. The experimental simulation, however, shows significant spatial variability, with large gradients over portions of the domain. The numerical difference between the control and experimental simulated sensible heat fluxes is shown in Fig. 9. Large differences in simulated sensible heat fluxes are seen over northern Texas and western Oklahoma, where the control experiment simulated sensible heat flux values are approximately 400 W m^{-2} greater than those in the experimental simulation. Large differences are also apparent over northeast Kansas.

Model-simulated surface latent heat flux values (W m^{-2}) are shown in Fig. 10. The control simulation produced little variation in latent heat flux, while the experimental simulation predicted much greater variation. Large heat flux gradients were simulated over portions of northern Texas in the experimental simulation. The numerical difference between the control and experimental simulated latent heat fluxes is shown in Fig. 11. Large differences are apparent over northern Texas and western Oklahoma, where the control experiment simulated latent heat flux values approximately 400 W m^{-2} greater than the experimental simulation. Smaller differences are seen over parts of Kansas and Nebraska, where simulated latent heat flux differences range from 150 to 200 W m^{-2}.

Boundary-layer-averaged wind velocity (m s^{-1}) and water vapor mixing ratio (g kg^{-1}) are shown in Fig. 12. Winds are southerly over much of the region in the control simulation, with a region of high water vapor mixing ratios and enhanced convergence over extreme

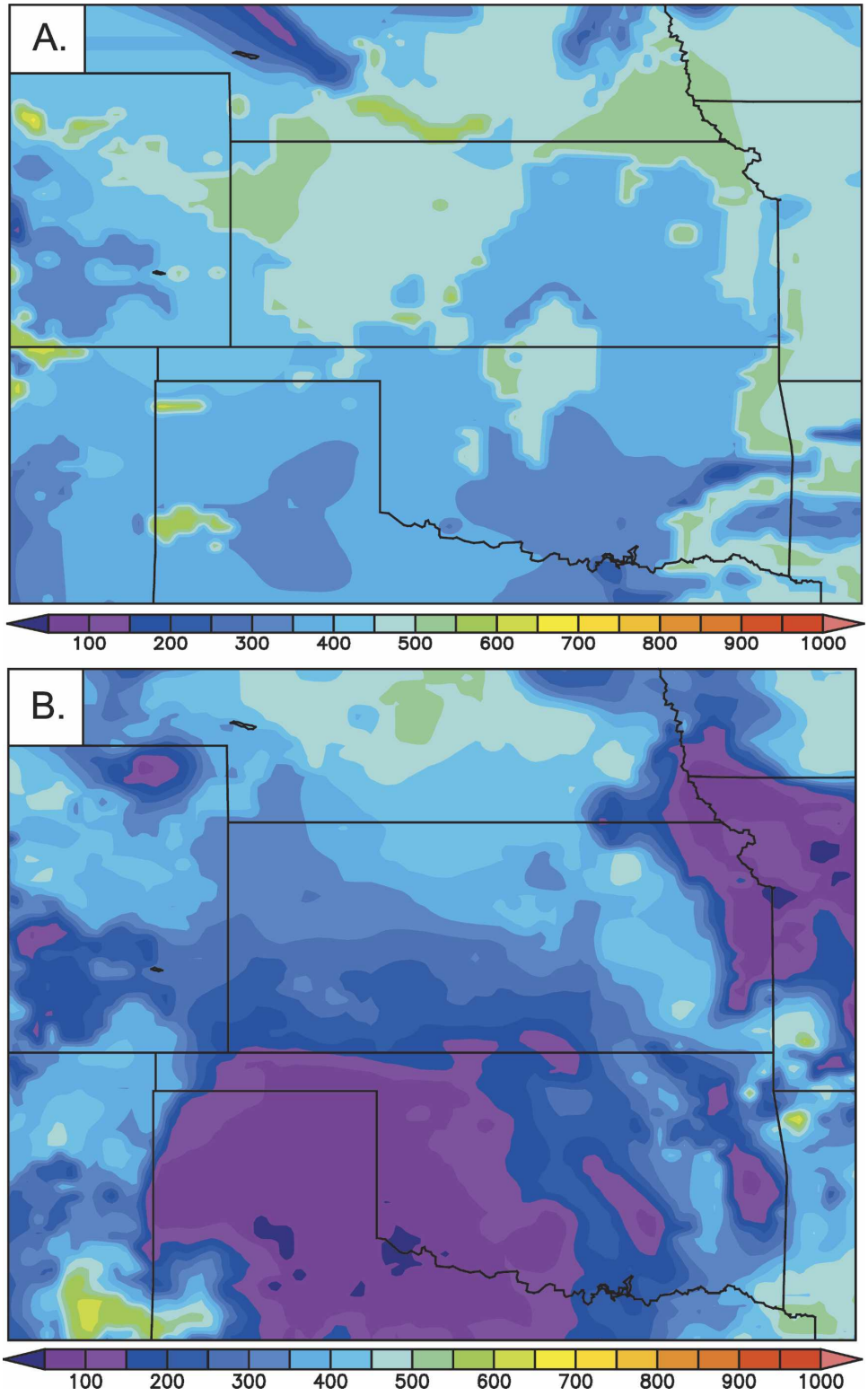

FIG. 10. (a) Control simulated surface latent heat fluxes (W m^{-2}) valid 0000 UTC 18 Jun 2002. (b) Experimental simulated surface latent heat fluxes (W m^{-2}) valid 0000 UTC 18 Jun 2002.

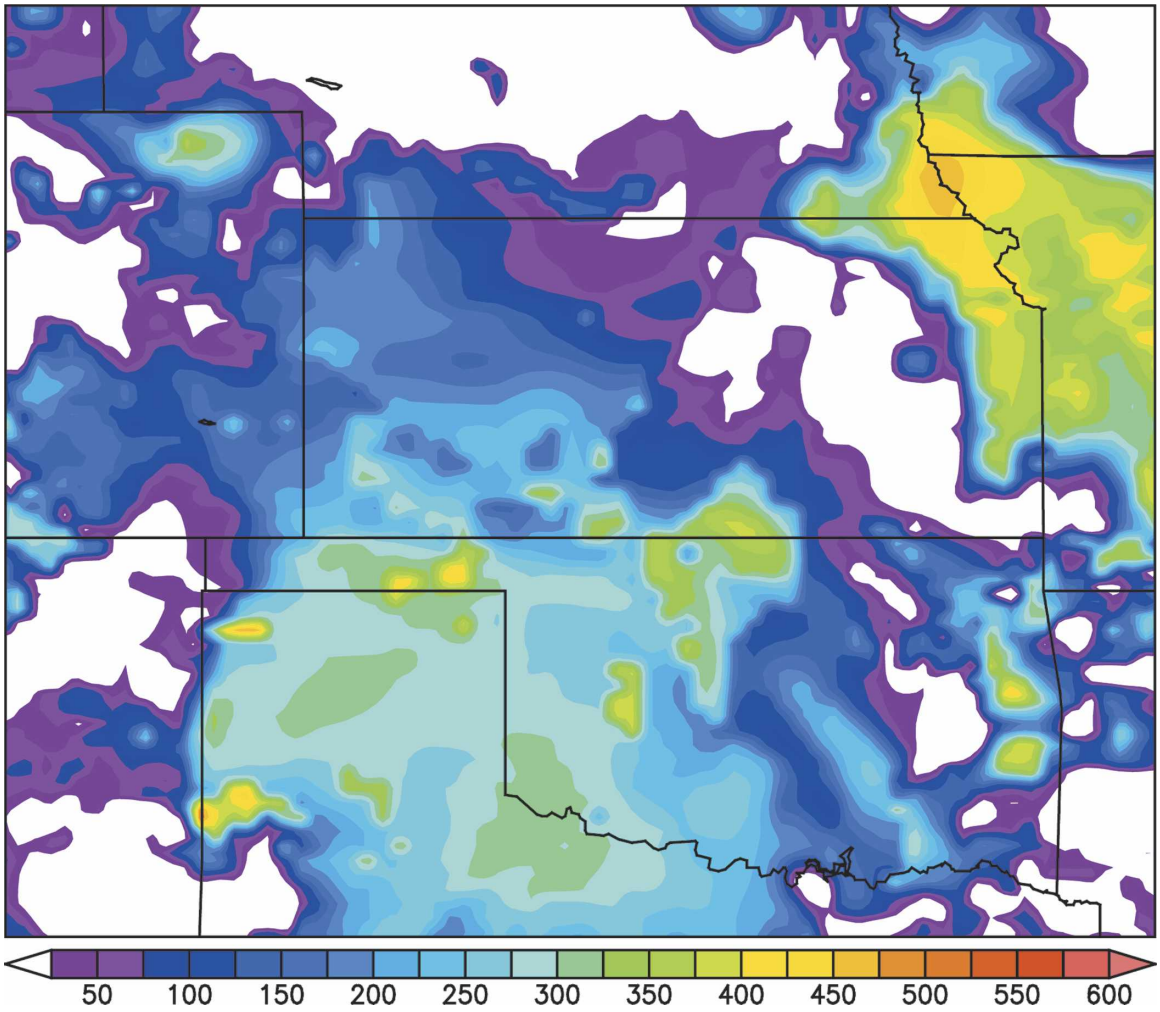

FIG. 11. Numerical difference between the control simulated surface latent heat flux and experimental simulated surface latent heat flux valid 0000 UTC 18 Jun 2002. Fluxes are shown in W m^{-2}.

western Oklahoma and Kansas. Boundary layer winds exhibit more variability in the experimental simulation, where simulated winds are easterly over much of central Oklahoma, southerly over much of western Oklahoma and Kansas, and northeasterly over northern Texas. Regions of high water vapor mixing ratios and enhanced convergence are seen over parts of northern Texas, as well as western and eastern Kansas in the experimental simulation. Although there is a decrease in the surface latent flux in the experimental simulation over parts of Kansas, Oklahoma, and northern Texas, a strong horizontal gradient is present, which causes strong low-level convergence accompanied by increase in moisture and vertical motion. The experimental simulation is in agreement with satellite (Fig. 3) and radar observations presented in Fig. 14 showing the occurrence of deep convection. The low-level wind pattern in the control simulation did not show this outflow pattern associated with deep convection.

Boundary layer vertical velocity (m s^{-1}) and relative humidity (% contoured) are shown in Fig. 13. With the exception of northeastern Kansas and western Oklahoma, the control simulated boundary layer relative humidity values are less than 60%. The control simulation also predicted several areas of weak vertical motion over eastern Kansas and eastern Colorado. The experimental simulation predicted high boundary layer relative humidity and moderate vertical motion in several regions, including eastern Kansas, western Oklahoma, and northern Texas. A region of enhanced vertical motion is simulated over northern Texas in the experimental simulation, which is not found in the control simulation.

Precipitation reflectivity (dBZ) is shown in Fig. 14.

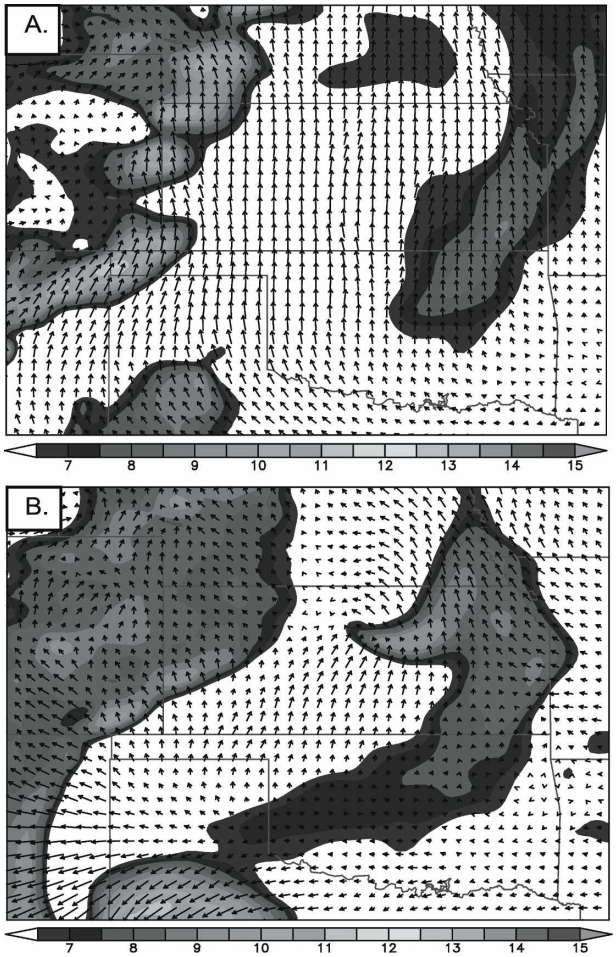

FIG. 12. (a) Control simulated boundary-layer-averaged wind velocity (m s^{-1}) and mixing ratio (shaded in g kg^{-1}) valid 0000 UTC 18 Jun 2002. (b) Experimental simulated boundary-layer-averaged wind velocity (m s^{-1}) and water vapor mixing ratio (shaded in g kg^{-1}) valid 0000 UTC 18 Jun 2002.

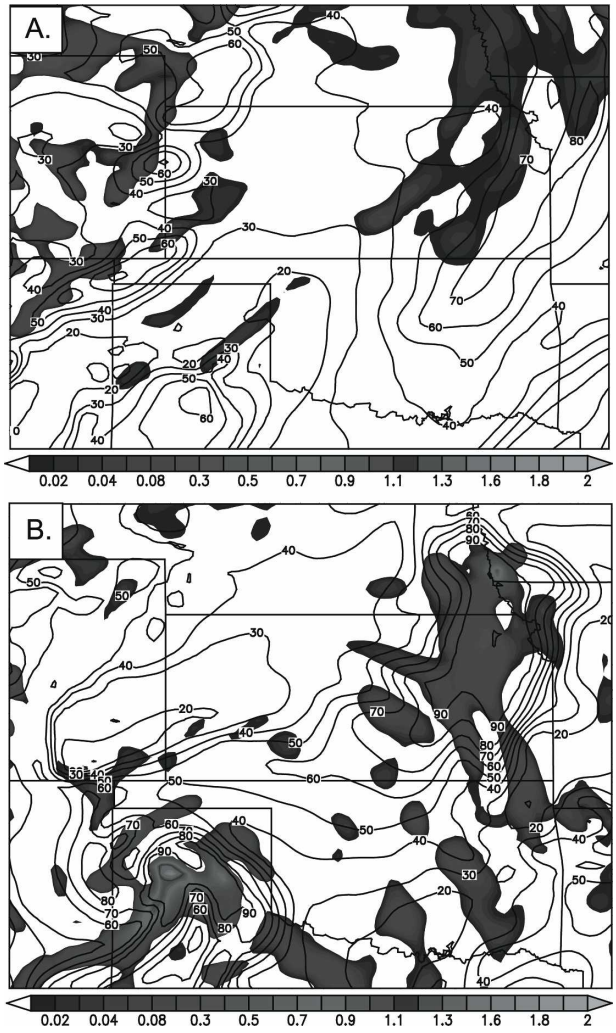

FIG. 13. (a) Control simulated boundary layer vertical velocity (shaded in m s^{-1}) and relative humidity (% contoured) valid 0000 UTC 18 Jun 2002. (b) Experimental simulated boundary layer vertical velocity (shaded in m s^{-1}) and relative humidity (% contoured) valid 0000 UTC 18 Jun 2002.

Control simulated reflectivity is shown in Fig. 14a, with experimental simulated reflectivity in Fig. 14B, and National Weather Service Doppler radar reflectivity in Fig. 14c. With the exception of eastern Nebraska, the control simulation did not predict any precipitation over the entire domain. The experimental simulation predicted two regions of significant precipitation: one in northern Texas and the other in southeastern Nebraska/southwestern Iowa into northeastern Kansas. Reflectivity data from National Weather Service Doppler Radar show intense precipitation over northern Texas and central Kansas, with lighter precipitation detected over northeastern Kansas and southeastern Nebraska. Neither simulation resolved the intense precipitation over central Kansas, although the experimental simulation predicted strong convection over north Texas and lighter precipitation over northeastern Kansas. Both simulations overpredicted precipitation in eastern Nebraska. As shown in Fig. 13b, high boundary layer relative humidity and enhanced vertical motion over northern Texas likely contributed to the increased convection in the experimental simulation.

Seventy-two-hour total precipitation (cm) valid 0000 UTC 17 June through 0000 UTC 20 June 2002 is shown in Fig. 15. Figure 15a is from the control simulation, while Fig. 15b is from the experimental simulation. Multisensor precipitation estimate (MPE) data over the study region is shown in Fig. 15c. MPE corrects radar precipitation estimates with observations from surface gauges. The control simulation predicted light precipitation (less than 1.25 cm) over much of central Nebraska and portions of New Mexico and heavier pre-

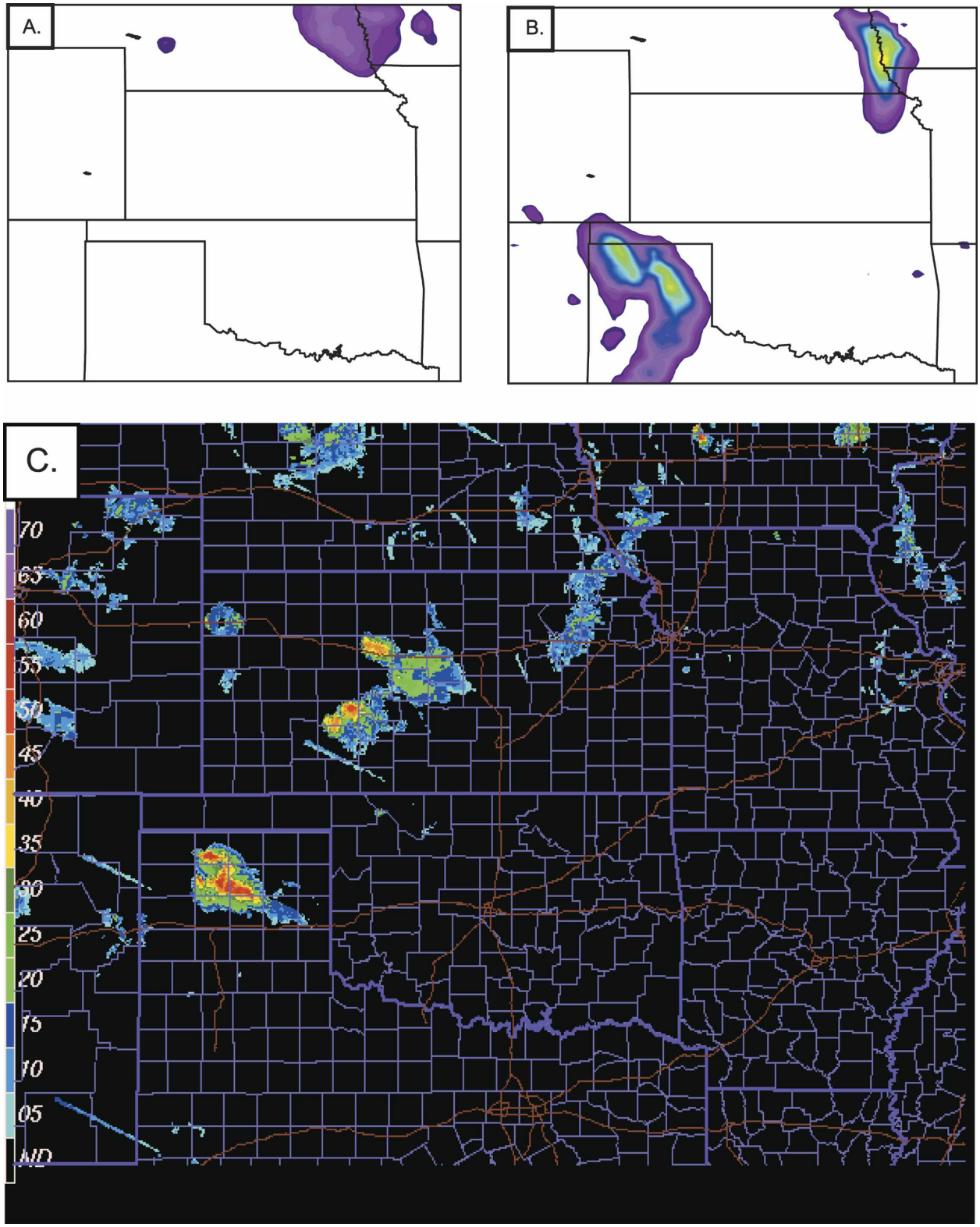

FIG. 14. (a) Control simulated reflectivity (dBZ) valid 0000 UTC 18 Jun 2002. (b) Experimental simulated reflectivity (dBZ) valid 0000 UTC 18 Jun 2002. (c) National Weather Service Doppler radar reflectivity (dBZ) valid 0000 UTC 18 Jun 2002.

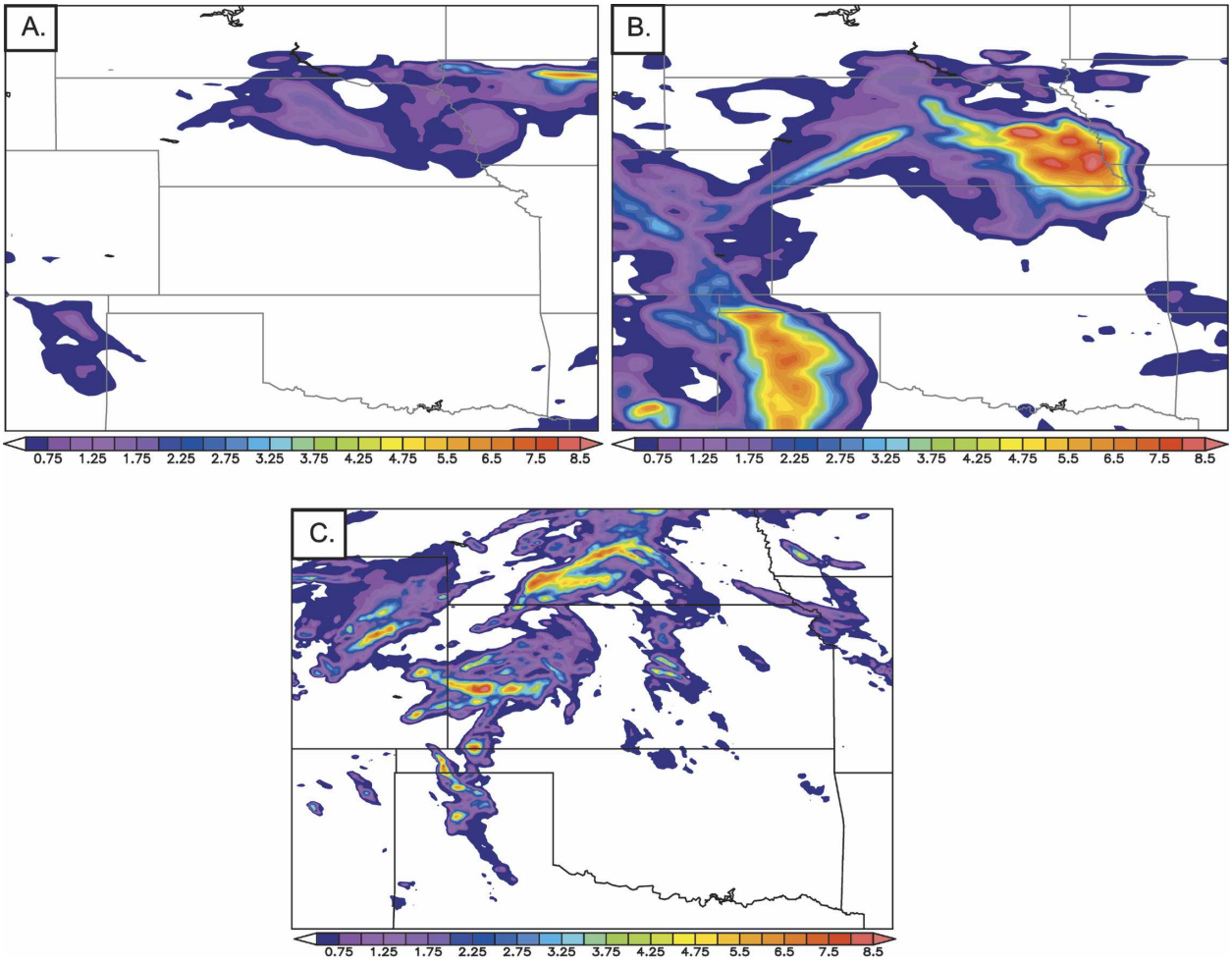

FIG. 15. Seventy-two-hour accumulated precipitation valid 0000 UTC 17 Jun–0000 UTC 20 Jun 2002: (a) control, (b) experimental, and (c) multisensor precipitation estimate.

cipitation (2.5–5 cm) over western Iowa. Less than 0.5 cm was simulated elsewhere in the domain. The experimental simulation predicted several regions of precipitation greater than 4 cm, including northern Texas and portions of central and eastern Nebraska into northeastern Kansas. MPE data show several regions of enhanced precipitation, including northern Texas, western Oklahoma, central and western Kansas, eastern Colorado, and portions of central Nebraska. The experimental simulation overpredicted the spatial coverage of precipitation over parts of the domain, including northern Texas, eastern New Mexico, eastern Colorado, northeastern Oklahoma, and Nebraska. However, the simulated precipitation amounts and distribution from the experimental simulation agreed more closely with MPE precipitation data than the control simulation. This is likely a result of the enhanced surface heat flux gradients in the experimental simulation driving more boundary layer moisture convergence, enhancing vertical motion, and inducing moist convection.

5. Conclusions

The main goal of this research is to study the effects of using the Flux-Adjusting Surface Data Assimilation System (FASDAS) on numerical simulations of convective initiation during the International H_2O Project (IHOP_2002) over the southern Great Plains (SGP) of the United States during June 2002. Two 72-h numerical simulations were performed. A control simulation was run that assimilated all available IHOP_2002 data into the standard MM5 four-dimensional data assimilation program. An experimental simulation was performed that assimilated all available IHOP_2002 data into the FASDAS version of the MM5.

Surface heat fluxes from the experimental simulation

agreed more closely with observations from Kansas and Oklahoma as compared to the control simulation. Intense surface heat flux gradients over portions of northern Texas and western Oklahoma were simulated by the experimental simulation. The control simulation predicted more uniform surface heat flux patterns over the region. Improved surface heat flux gradients in the experimental simulation likely enhanced simulated boundary layer moisture convergence. Enhanced moisture convergence increased boundary layer relative humidity and vertical motion, which led to the development of deep, moist convection. The control experiment simulated much weaker surface heat flux gradients, which likely resulted in the lack of simulated deep convection over the region during this study period. Future research would include a more detailed statistical evaluation of the FASDAS scheme, including several simulations over the southeastern United States.

Acknowledgments. This work was supported by the Atmospheric Sciences Division, National Science Foundation, under the Grant ATM-0233780 and by the State Climate Office of North Carolina. Access to the IHOP_2002 Hourly Surface Meteorological Composite data was provided by Steve Williams at UCAR. The authors thank Dr. Francois Bouttier and the anonymous reviewer for several helpful suggestions.

REFERENCES

Alapaty, K., D. S. Niyogi, and M. Alapaty, 2001a: Indirect assimilation of soil moisture availability in the MM5. *Proc. 11th Penn State/NCAR MM5 Users' Workshop,* Boulder, CO, Pennsylvania State University/NCAR. [Available online at http://www.mmm.ucar.edu/mm5/workshop/ws01/alapaty2.pdf.]

——, N. L. Seaman, D. S. Niyogi, M. Alapaty, G. Hunter, and D. Stauffer, 2001b: Evaluation of a Surface Data Assimilation technique using the MM5. *Proc. 11th Penn State/NCAR MM5 Users' Workshop,* Boulder, CO, Pennsylvania State University/NCAR. [Available online at http://www.mmm.ucar.edu/mm5/workshop/ws01/alapaty3.pdf.]

——, ——, ——, and A. F. Hanna, 2001c: Assimilating surface data to improve the accuracy of atmospheric boundary layer simulations. *J. Appl. Meteor.,* **40,** 2068–2082.

Anthes, R., 1974: Data assimilation and initialization of hurricane prediction models. *J. Atmos. Sci.,* **31,** 702–718.

Betts, A. K., F. Chen, K. E. Mitchell, and Z. Janjić, 1997: Assessment of the land surface and boundary layer models in two operational versions of the NCEP Eta Model using FIFE data. *Mon. Wea. Rev.,* **125,** 2896–2916.

Bouttier, F., J.-F. Mahfouf, and J. Noilhan, 1993: Sequential assimilation of soil moisture from low-level atmospheric parameters. Part II: Implementations in a mesoscale model. *J. Appl. Meteor.,* **32,** 1352–1364.

Chen, F., and J. Dudhia, 2001: Coupling an advanced land surface–hydrology model with the Penn State–NCAR MM5 modeling system. Part I: Model implementation and sensitivity. *Mon. Wea. Rev.,* **129,** 569–585.

Ek, M., K. Mitchell, E. Rogers, T. Black, G. Gayno, F. Chen, and J. Kim, 2003: Upgrades to the unified Noah land-surface model in the operational NCEP mesoscale Eta Model. Preprints, *17th Conf. on Hydrology,* Long Beach, CA, Amer. Meteor. Soc., CD-ROM, 3.9.

Kain, J. S., 2004: The Kain–Fritsch convective parameterization: An update. *J. Appl. Meteor.,* **43,** 170–181.

Kistler, R. E., 1974: A study of data assimilation techniques in an autobarotropic primitive equation channel model. M.S. thesis, The Pennsylvania State University, 84 pp.

Mahfouf, J. F., 1991: Analysis of soil moisture from near surface parameters: A feasibility study. *J. Appl. Meteor.,* **30,** 1534–1547.

Stauffer, D. R., and N. L. Seaman, 1990: Use of four-dimensional data assimilation in a limited-area mesoscale model. Part I: Experiments with synoptic-scale data. *Mon. Wea. Rev.,* **118,** 1250–1277.